DEVELOPMENT OF LIDAR MEASUREMENT SIMULATOR CONSIDERING TARGET SURFACE REFLECTION

Yu Nakajima[(1)], Takahiro Sasaki[(1)], Naoki Okada[(1)], Toru Yamamoto[(1)]

[(1)] Japan Aerospace Exploration Agency, 2-1-1 Sengen, Tsukuba, Ibaraki, Japan 305-9505, Email:nakajima.yu@jaxa.jp

ABSTRACT

A LiDAR simulator to emulate on-orbit observation data was developed to verify LiDAR navigation algorithms. The simulator emulates measured distance and intensity of a target, considering LiDAR scanning patterns. The BRDF of major materials on the debris surface was obtained from the experiment. The obtained BRDF table data were fitted to a modified Phong model to emulate signal strength under arbitrary conditions. Measurement errors on each material were also experimentally obtained and modeled. The errors were divided into bias and random errors, and then emulated in the simulator. The LiDAR simulator can generate pseudo-observation data by simulation, which enables the user to test LiDAR navigation algorithms with various conditions.

1 INTRODUCTION

Space debris has been increasing drastically due to recent space development. In 2009, an operating satellite and a used rocket body actually crashed on-orbit, resulting in loss of the satellite and the dispersion of many fragments. The so-called “Kessler syndrome” thus came into effect. One study has revealed that removing five large-scale debris from a crowded orbit is effective in curtailing the proliferation of space debris [1].

Most of the space debris found on-orbit are used rocket bodies and satellites [2]. The target can be either rocket bodies or un-operating satellites. This study focused on the used rocket bodies, given their similar structures. Conversely, satellites usually have a distinctive appearance depending on their missions. The rendezvous with and capture of a debris depends on its shape and appearance, as it is easy to adopt the technique to other targets if their structures and appearance are similar. For this reason, the used rocket body was chosen in this study as the target debris.

One major difficulty in achieving active debris removal is rendezvous with a target debris on-orbit. Unlike a cooperative target such as the ISS, debris objects have no markers to facilitate the chaser’s relative navigation. LiDAR is one of the candidate sensors for relative navigation against target debris. In general, LiDAR emits laser light and measures the reflection with a detector to measure a round-trip time, which can be converted to distance. This feature enables the chaser to obtain the distance from a target without onboard image processing, which is necessary for optical cameras.

However, testing LiDAR on the ground is difficult because a full-scale test is required to evaluate measurement errors. Navigation sensors are commonly tested with a scale model. The model is easy to handle and can obtain much data under various conditions. Therefore, the scale model is used to evaluate optical cameras. However, a major difference from on-orbit data is that a scale test also scales the measurement errors and resolution of LiDAR.

A target of a full-scale test is quite large when attempting to remove a large-scale debris. This is difficult to handle and obtaining much data under various conditions is unrealistic. Figure 1 shows an example scene of a full-scale test in the laboratory. Moreover, the larger the target, the larger the supporting jigs. The jigs and surrounding obstacles usually enter the LiDAR field of view, as shown in Fig. 2. LiDAR output contains not only the target but also the wall, hanging jigs, and other obstacles in the laboratory. They cause multipath that never occurs on-orbit. Moreover, such obstacles are not observed on-orbit and thus should be eliminated from the data prior to the evaluation, which is not an easy task.

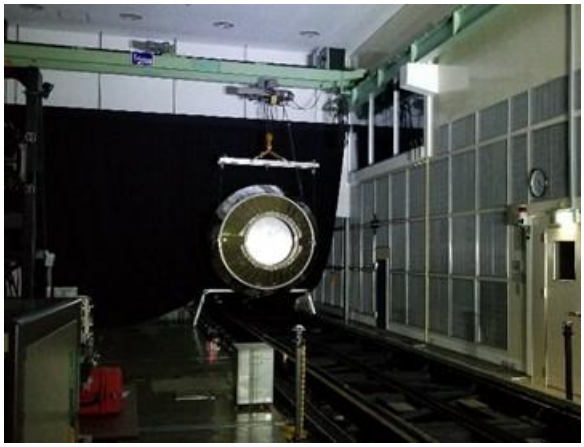

Figure 1. Full-scale Experiment in the Laboratory

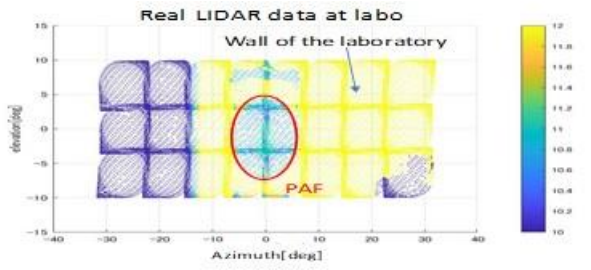

Figure 2. Real LiDAR Data Obtained in the Laboratory

The evaluation of LiDAR measurement and navigation algorithms with various conditions requires a LiDAR simulator that can emulate on-orbit LiDAR measurement. As LiDAR measures distance by observing laser light reflected from the target, reflection on the target surface is one of the key factors. In addition, measurement errors have a correlation to reflection intensity. For these reasons, the light reflection intensity of major surface materials on a debris is experimentally obtained and the Bidirectional Reflectance Distribution Function (BRDF) was observed. The observed BRDF data were fitted to a modified Phong model. By using this model, the simulator can reproduce the signal intensity.

There is a strong demand for simulating LiDAR, particularly in the self-driving car industry [3,4]. Many researchers work on this topic, but weather (such as humidity) and overall data outlook are their main concerns, since their final goals are avoiding a clash with obstacles, and are less interested in detecting the attitude of obstacles. However, in rendezvous with space debris, precise high precision attitude and distance information are essential to capture debris. For these reasons, there is an urgent demand for a LiDAR simulator to emulate the observation data on-orbit.

In the field of space, navigation algorithms using LiDAR have been widely researched [5,6], although such studies verified their proposed approach with full simulation without modeling errors. Capturing a debris requires cm-order precise relative control; therefore, such errors should be modeled according to LiDAR and emulated in the simulation.

2 SIMULATOR OVERVIEW

The goal of this research is to develop a LiDAR simulator that can emulate on-orbit LiDAR data as precisely as possible. This will help to develop navigation algorithms by providing LiDAR measurements under various conditions. The expected features are as follows:

- emulating measured distance including errors
- emulating intensity and observability of the target
- modeling of the LiDAR scanning pattern

Figure 3. Cepton Vista P-60 [7]

Table 1. Key Specifications of Cepton Vista P-60

Item	Specification
Range	200 m @ 30% reflectivity
FOV	60° x 22°
Angular resolution	0.25° x 0.25°
Size	102 x 58 x 101 mm, 0.9 kg

For instance, a Cepton Vista P-60 was modeled in this research. Figure 3 shows the appearance of this LiDAR, and Table 1 lists its specifications.

Because this LiDAR was selected as an example application, subsequent discussion focuses on the Cepton Vista P-60, but is applicable to other LiDARs as well. Simulator inputs are time, relative position/attitude, and target shape, while it outputs time, distance, azimuth/elevation angle, and intensity. In order to emulate those outputs, a simulator consisting of four modules (scanning model, geometric model, radiometric model, detection model) was proposed. Modeling laser intensity received at the LiDAR is a key technique to precisely emulate the LiDAR output. The signal strength is related to measurement accuracy. Moreover, weak signal reflection will not be detected by a detector and point data will be missing. In order to emulate the missing data, signal intensity must be modeled.

3 SCANNING MODEL

LiDAR scanning patterns are generally unique to the model. The Cepton Vista P-60 also has a unique scanning pattern. The scanning pattern is an 8 by 3 arrayed Lissajous-like curve. Each Lissajous scanning pattern overlaps at the edge; therefore, the scanning pattern has a lattice-like shape. The density of scanning rays is biased and not evenly distributed, so it is important to model the scanning pattern to evaluate the LiDAR navigation algorithms. The frequency of the Lissajous curve was obtained thorough the experimentally obtained data and the modeled scanning pattern. Figure 5 shows the scanning pattern obtained by the Cepton Vista P-60; Fig. 6 shows the scanning pattern emulated by the simulator.

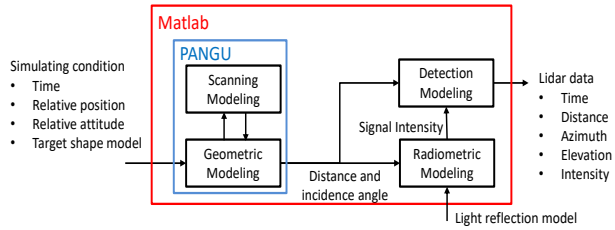

Figure 4. Overview of Simulator

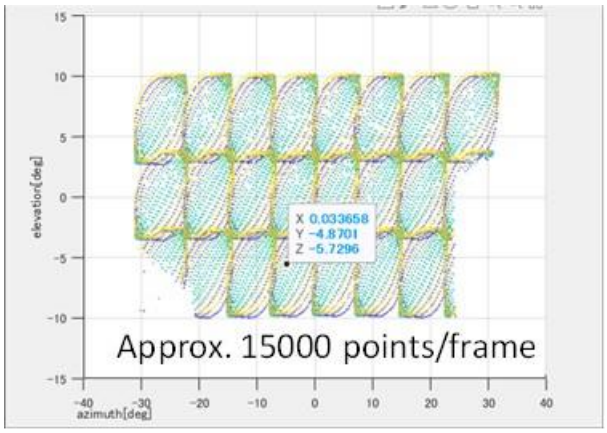

Figure 5. Cepton Vista P-60 Scanning Pattern

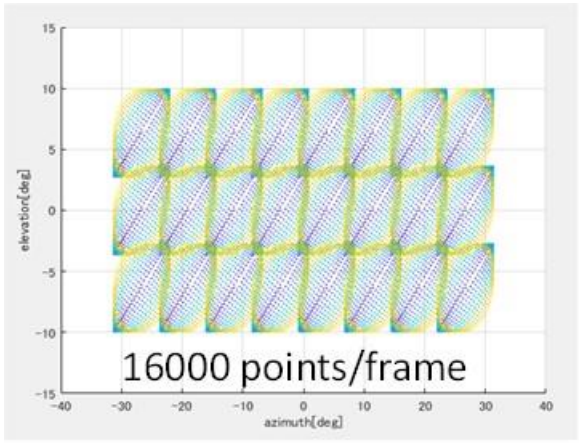

Figure 6. Scanning Pattern by LiDAR Simulator

4 GEOMETRIC MODEL

Overall simulation is conducted by MATLAB. However, geometric model of the LiDAR was simulated by PANGU [8]. This software was originally developed to emulate the optical image of spacecraft and planets obtained by cameras. In addition, this software has a function to calculate a distance and incidence angle of LiDAR measurement. Both the distance and incidence angle are true value and no errors are modeled. Therefore, we use this tool to obtain tool distance and add measurement errors modeled from the experimental results.

5 REFLECTION MODEL

Modeling laser intensity received at the LiDAR is a key technique to precisely emulate the LiDAR output. The signal strength is related to measurement accuracy. Moreover, weak signal reflection will not be detected by a detector and point data will be missing. In order to emulate the missing data, signal intensity must be modeled.

The laser reflection on the surface of the debris differs depending on the materials. Six major material samples on the rocket body are obtained and its optical characteristics are evaluated. Figure 7 shows the six evaluated materials. Poly Isocyanate Foam (PIF) has an uneven surface and Multi-Layer Insulation (MLI) is a mirror-like soft material that strongly reflects light. These two materials account for most of the rocket surface. The head parts consist of the Payload Attachment Fitting (PAF), Payload Support Structure (PSS), bulkhead, and adapter. These four materials have metallic characteristics.

Laser luminance [w/srm^2] can be obtained as:

$$L_{laser} = f_{BRDF} \cdot E_{laser} \cdot \cos\theta_o, \quad (1)$$

where laser illuminance E_{laser} [w/m^2] is obtained by

$$E_{laser} = P_o \tau_t / \pi \left(\frac{r\Delta\theta}{2}\right)^2. \quad (2)$$

Then received signal power [w] is derived by

$$P_r = L_{laser} \tau_r A(r) \cos\theta_o \cdot 4\pi \frac{\pi(D/2)^2}{4\pi r^2}. \quad (3)$$

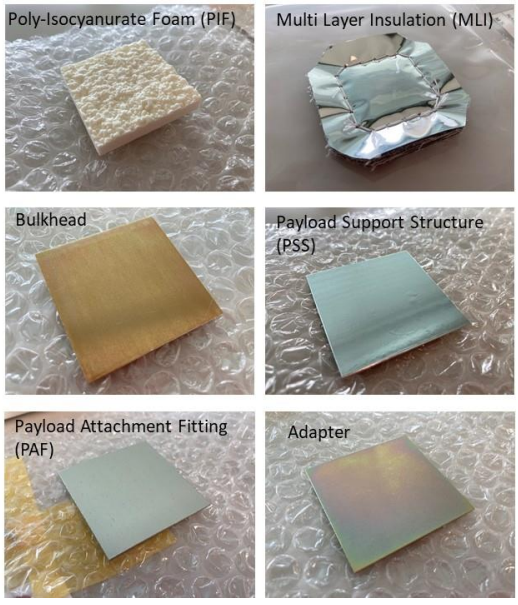

Figure 7. Major Materials of a Rocket Surface

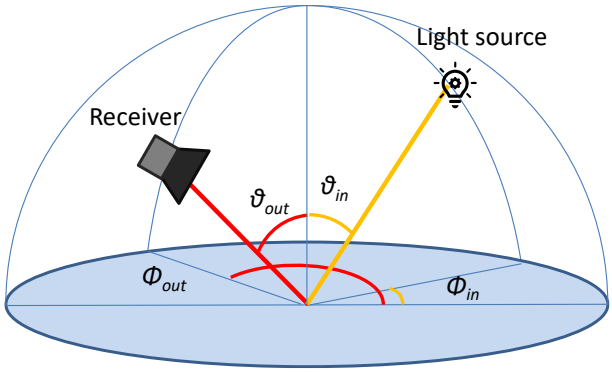

Figure 8. Bidirectional Reflectance Distribution Function

Laser light reflection on the surface of each material is evaluated by the Bidirectional Reflectance Distribution Function (BRDF) [8]. BRDF is a function of four variables (θin, φin, θout, φout) that defines how light is reflected at an opaque surface. The function takes an incoming light direction (θin, φin) and an outgoing direction (θout, φout), and returns the ratio of reflected radiance exiting along with the irradiance incident on the surface. Figure 8 illustrates the concept. The function can be expressed as Eq. (4) below.

$$f_{brdf}(\theta_{in}, \varphi_{in}, \theta_{out}, \varphi_{out}) = \frac{L_{receive}}{L_{emit} cos\theta_{in} d\omega_{in}} \quad (4)$$

We can evaluate the reflection with BRDF, by changing input parameters $\theta_{in}, \varphi_{in}, \theta_{out}, \varphi_{out}$ and observing the ratio of emitter and receiver light luminance. We took data on the basis of five degrees for each $\theta_{in}, \varphi_{in}, \theta_{out}, \varphi_{out}$ and created a data table. Figure 9 shows the obtained data. PIF showed diffusive reflection, while the other materials showed specular reflection. MLI and the PSS have strong specular reflection characteristics. The PSS, bulkhead, and adapter showed anisotropic reflection, but are modeled as isotropic with averaged data to reduce computation time.

The obtained data were fitted to a modified Phong reflectance model [9]. This model considers diffuse and specular characteristics of the material expressed as

$$f_{BRDF} = \frac{k_d}{\pi} + \frac{k_s(n+2)}{2\pi} cos^n(\alpha), \quad (5)$$

where α is the angle between the perfect specular reflective direction and outgoing direction. n is a specular exponent to express the sharpness of specular reflections. k_d and k_s denote diffuse reflectivity and specular reflectivity. By choosing these parameters, any combination of diffuse reflection and specular reflection can be expressed. Five types of materials account for most of the rocket body surface: PAF, PSS, MLI, PIF, and engine nozzle. The bulkhead and adapter were not modeled due to their smaller surface areas. The light reflection of those five materials were experimentally observed to determine reflection parameters described above. Figure 10 shows the fitted modified Phong models.

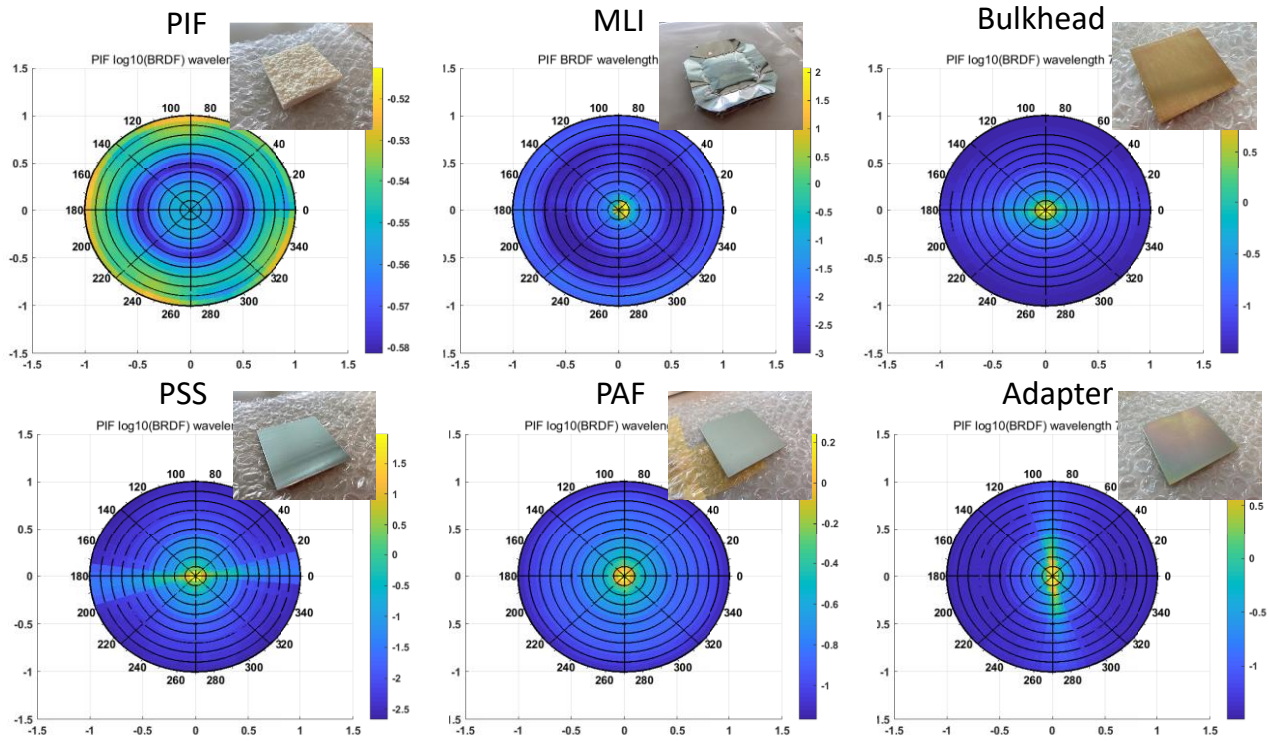

Figure 9. BRDF with Incidence Angle of 0 Degrees

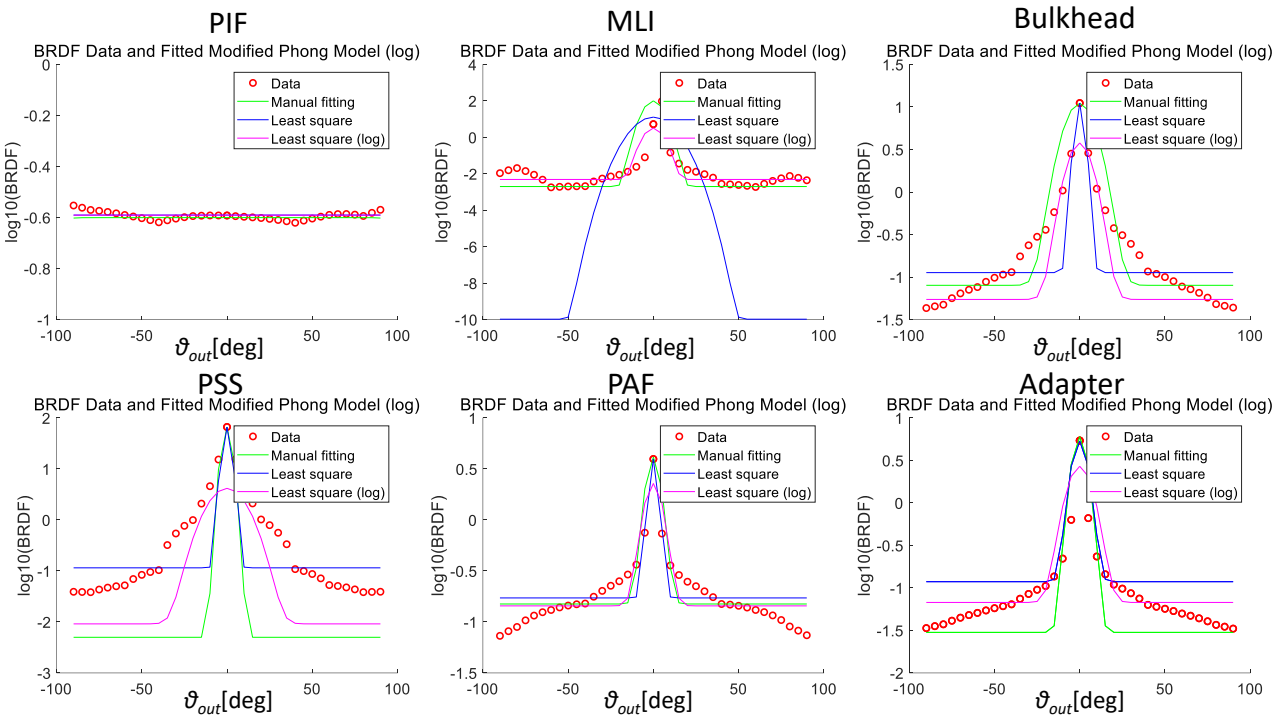

Figure 10. BRDF Result vs Modified Phong Model

The red circles indicate the BRDF data obtained by the experiment. The pink and blue lines indicate the least square fit results. Specifically, the blue line indicates the least square fit results of the true BRDF, and the pink line denotes those of the logarithm BRDF. Since the modified Phong model is a simple model with three parameters, it is thus difficult to model the experimentally obtained BRDF data with high precision. This model expresses the overall characteristics of the BRDF, while some differences were found on the edge of the data apart from the peak. Although more precise models may be considered, a modified Phong model was adopted in this study for quicker computation. Thus, the simulator emulates laser light reflection by using the modified Phong model with each material parameter.

6 DETECTION MODEL

The detection model module emulates the distance measurement error under various distance and attitude conditions. To model the error, relative distance from LiDAR to the target was measured in the laboratory with various distances and attitudes of the target. Figure 11 shows the experiment changing relative distance; Fig. 12 shows the experiment changing relative attitude.

The solar light simulator is set to model solar disturbances. Bias and random errors are obtained from 20 frames of the LiDAR data. The obtained bias and random errors are considered in the measurement model of the simulator.

The distance has been changed from 2 m to 25 m and attitude was changed from 0 degrees to 80 degrees. Table 2 lists the data obtained at 5 m and at 15 m. The data listed show the bias and random errors of six materials. The table suggests the following:

- Almost no difference in measurement error was observed between 5-m and 15-m distances.
- Bias errors were different among materials, while random errors of each material were similar.

In order to emulate the characteristics mentioned above, the simulator is set as follows:

- Setting distance error regardless of actual distance
- Setting bias/random errors depending on the materials

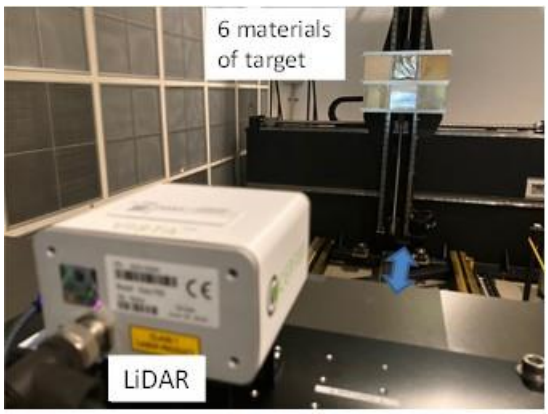

Figure 11. Measurement Experiment Changing Distance

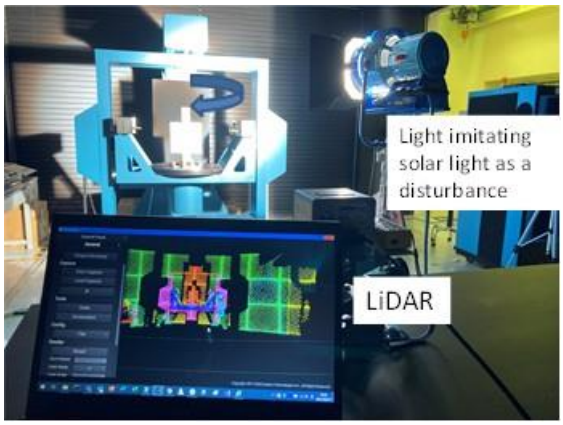

Figure 12. Measurement Experiment Changing Attitude

Table 2. Measurement Errors

Condition	Error		
5 m Bias [m]	PIF -0.1417	MLI -0.1361	Bulkhead -0.1334
	PSS -0.1179	PAF -0.1146	Adapter -0.1329
5 m Random (1σ) [m]	PIF 0.0228	MLI 0.0228	Bulkhead 0.0306
	PSS 0.0357	PAF 0.0437	Adapter 0.0338
15 m Bias	PIF -0.1349	MLI -0.1337	Bulkhead -0.1093
	PSS -0.1053	PAF -0.1199	Adapter -0.1304
15 m Random (1σ) [m]	PIF 0.0334	MLI 0.0387	Bulkhead 0.0344
	PSS 0.0390	PAF 0.0472	Adapter 0.0393

7 SIMULATOR OUTPUT

Figure 13 shows an example of LiDAR simulator output. This image is a three-dimensional plot of LiDAR measurement 10 m from the target debris. The signal reflection intensity at each point is calculated, and if the intensity is below a certain threshold or saturated, the point data is omitted. Point clouds are broadcast unevenly due to the LiDAR's scanning pattern. The distance to the debris was reconstructed as data taken by real LiDAR.

Figure 14 shows the distance data observed 10 m from the debris. The scanning pattern was clearly traced, and a lattice-like pattern was observed. In addition, the surface materials were classified into five parts as shown in Fig. 15. The distance errors are calculated by materials and added to the results shown in Figs. 13 and 14. The signal strength was weak, thereby making it difficult to discuss the characteristics, but it has strong reflection, especially on MLI facing the LiDAR. The specular reflection on the surface of the rocket body was modeled and emulated.

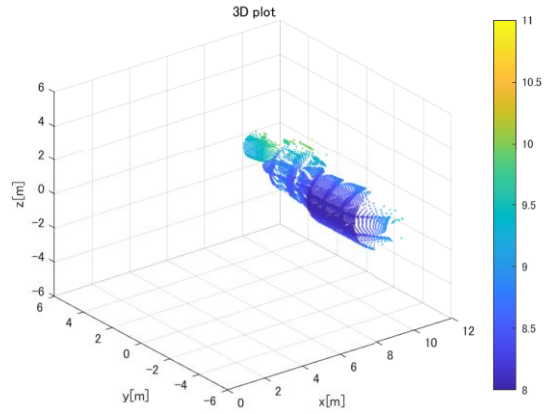

Figure 13. Simulated LiDAR Measurement from 10m

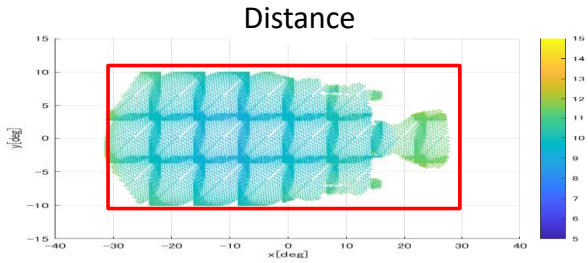

Figure 14. Distance Results

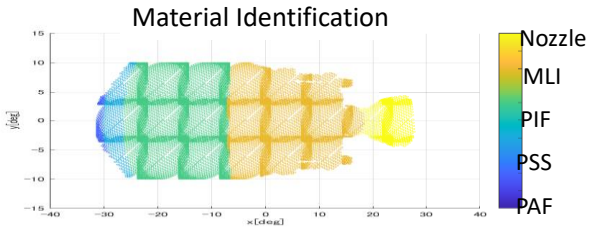

Figure 15. Surface Materials Identification

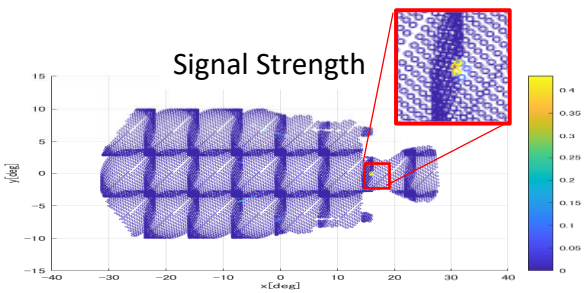

Figure 16. Signal Intensity

For a comparison, a full-scale model experiment was also

conducted using the Payload Attachment Fitting (PAF) of the rocket body. The PAF was hung in the laboratory and experimental data was taken by the Cepton Vista P-60 LiDAR. Figure 1 shows the PAF hung in the laboratory.

Figures 17 and 18 show the LiDAR simulator data and real LiDAR data obtained in the laboratory, respectively. In the experiment, only the PAF and its surrounding parts were observed by LiDAR, and not the entire rocket body. However, the observed PAF was similar to that emulated by the proposed LiDAR simulator.

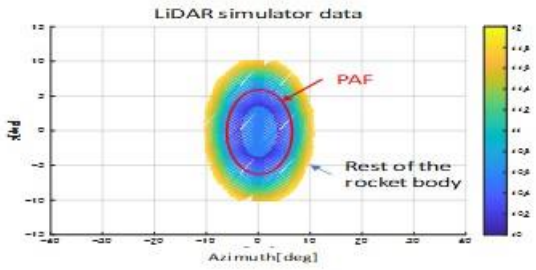

Figure 17. LiDAR simulator data

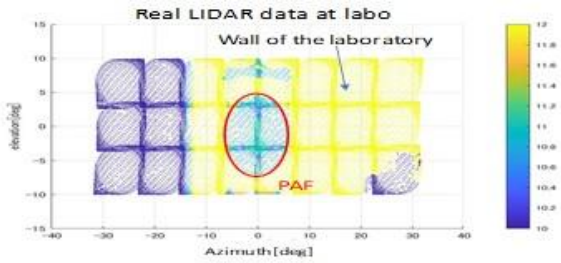

Figure 18. Real LiDAR data by Cepton Vista P-60

8 CONCLUSION AND FUTURE WORK

A LiDAR simulator was researched to evaluate LiDAR without using a full-scale debris model. The simulator can emulate on-orbit LiDAR data. This simulator emulates measured distance and intensity, considering LiDAR scanning patterns. Measurement errors on each material were experimentally analysed and modeled. The errors were divided into bias and random errors, and then emulated in the simulator. The BRDF of each material was analysed from the experiment. The BRDF table data obtained were fitted to a modified Phong model to emulate signal strength under any condition. The LiDAR simulator can generate pseudo-observation data by simulation, which enables the user to test LiDAR navigation algorithms under various conditions. As future work, modeling solar light as a disturbance would be ideal.

REFERENCES

1. Inter-Agency Space Debris Coordination Committee, Working Group 2 (2013) *Stability of the Future LEO Environment*. Tech. Rept. Rev. Jan. 2013.
2. J.-C. Liou (2011) *Orbital Debris and Future Environment Remediation*. OCT Technical Seminar NASA HQ, Washington DC.
3. A. Dosovitskiy, G. Ros, F. Codevilla, A. Lopez and V. Koltun (2017) *CARLA: An Open Urban Driving Simulator*. 1st Conference on Robot Learning.
4. S. Bechtold and B. Hofle (2016) *HELIOS: A Multi-purpose LiDAR Simulation Framework for Research, Planning and Training of Laser Scanning Operations with Airborne, Ground-based Mobile and Stationary Platforms.* ISPRS Annuals of the Photogrammetry, Remote Sensing and Spatial Information Sciences, Vol. III-3.
5. A. Nocerino, R. Opromolla, G. Fasano and M. Grassi (2020) *Analysis of LiDAR-based relative navigation performance during close-range rendezvous toward an uncooperative spacecraft.* IEEE 7th International Workshop on Metrology for AeroSpace (MetroAeroSpace), Pisa, Italy, pp. 446-451.
6. Taati, B., Shyr, A. and Little, J. (2005) Satellite Pose Acquisition and Tracking with Variable Dimensional Local Shape Descriptors.
7. https://www.cepton.com/products/vista-p
8. Rowell, N., Parkes, S., Dunstan, M., and Dubois-matra, O. (2012). *PANGU: VIRTUAL SPACECRAFT IMAGE GENERATION*.
9. F. E. Nicodemus (1965) *Directional reflectance and emissivity of an opaque surface*. Appl. Opt. 4, pp. 767.
10. Lafortune, E. P. and Willems, Y. D. (1994) Using the Modified Phong Model for Physically Based Rendering. pp. 1-19.